PERFORMANCE COMPARISON AND STABILITY CHARACTERIZATION OF TIMING AND GEODETIC GPS RECEIVERS AT IEN

R. Costa, D. Orgiazzi, V. Pettiti, I. Sesia, P. Tavella

Istituto Elettrotecnico Nazionale "Galileo Ferraris", Strada delle Cacce 91, Torino, Italy, metf@ien.it

Keywords: geodetic GPS receivers, stability, outliers, precise point positioning, time scale comparison.

Abstract

In this paper the noise characterization of the GPS receivers (both timing and geodetic) hosted at the Time and Frequency Laboratory of the Istituto Elettrotecnico Nazionale (IEN) "Galileo Ferraris" was taken into account. In particular, a specific algorithm as well as two different approaches (a classical GPS "common view" technique and a geodetic-based Precise Point Positioning, PPP) employed to process the data coming from such receivers were described.

Moreover, the paper focused on the preliminary timing performance of the PPP geodetic method by comparing them with the International GPS Service (IGS) estimates on the link between two European metrological institutes, such as IEN and PTB (Physikalisch-Technische Bundesanstalt), Braunschweig, Germany.

1 Introduction

The Time and Frequency Laboratory of the Istituto Elettrotecnico Nazionale (IEN) "Galileo Ferraris", Turin (Italy) is currently operating a 3S Navigation (in the following 3SN) multi-channel single-frequency GPS/GLONASS timing receiver performing "common view" measurements [1], allowing time scale comparisons with other remote UTC(k) laboratories. A second timing receiver of the same type, a TTS-2 with temperature stabilized antenna (in the following named TTS), is also working since mid December 2003.

In addition, two dual-frequency geodetic GPS receivers are available in a very short baseline set up. An Ashtech Z-12T "Metronome" receiver (hereafter named ASH) has been working since 2001, with external time and frequency reference signals directly connected to the national time scale UTC(IEN). This receiver, differentially calibrated in the context of an international campaign arranged in 2001 by BIPM, is now involved in the BIPM TAI P3 activities [5],[6].

Starting from March 2003 a second geodetic GPS receiver, a Javad Legacy with timing option (in the following JAV), is also operated. In the framework of the Galileo System Test Bed V1 (GSTB V1) [7], the first experimental phase of the Galileo project supported by the European Space Agency, this receiver is part of the Experimental Precise Timing Station (E-PTS), implemented at IEN in collaboration with Alenia Spazio, Roma (Italy), with the aim to generate and disseminate the Experimental Galileo System Time for the whole experimentation period planned for 2004.

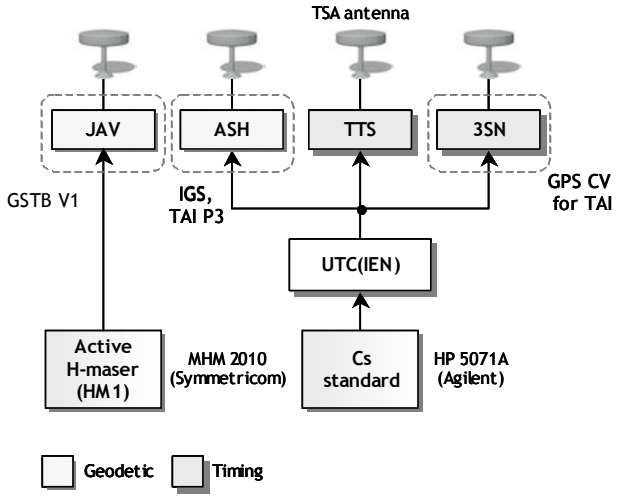

Figure 1: Timing and geodetic GPS receivers configuration at IEN Time and Frequency Laboratory.

First, in a "common view" approach relying on the measurements provided by all the GPS receivers (performed on either single or dual GPS frequencies), short and long term monitoring of the timing performance is routinely carried out by IEN, mainly focusing on the estimation of the noise and the stability of the equipment. In particular, the handling of measurement outliers as well as the data smoothing techniques are addressed with the aim of improving the robustness of the data processing. Real data sets were used, dealing with the influence of outliers and discussing the effectiveness of the Hampel filter (based on outlier-resistant median) as an outlier identification method.

Moreover, some additional efforts have been devoted to test the clock offset estimates obtained by Precise Point Positioning (PPP), as provided from the service kindly supplied by the Geodetic Survey Division (GSD) of Natural Resources, Canada (NRCan) [10]. This geodetic approach is based on high-quality GPS products (precise satellite orbits

and clocks) made available in near real time by the International GPS Service (IGS) [9]. From a first evaluation, this method seems to provide stability performance even better than that provided by a "common view" approach, mainly due to the use of both carrier phase measurements and high quality IGS products. Preliminary "timing" performance of this method are presented and discussed in this paper.

Besides, since January 2004 the Ashtech Z-12T receiver is qualified as an IGS station and the clock driving the receiver is thus estimated by the IGS via a carrier phase technique [15],[16]. A preliminary comparison of such estimates with respect to those coming from a PPP reduction is also reported in the paper.

2 Robust outliers detection algorithm

The computation of the time offset between the local UTC(k) and both GPS time and other remote time scales is one of the major duty of each metrological institute.

At the Time and Frequency Laboratory of IEN, this task is carried out by processing the GPS receivers data through a specific three-stages algorithm, which has the main aim to detect and remove any outliers and to provide robustly smoothed estimates.

At first, starting from the CGGTTS-formatted (Common GPS GLONASS Time Transfer Standard) [2], measurement data collected at IEN (3SN receiver), a MAD (Median of the Absolute Deviation) based filtering procedure is performed with the aim of removing outliers caused mainly by unhealthy satellites or less favourable geometric conditions. Such a filter is applied on the set of all the measurements concerning the satellites in view at each epoch, in order to detect outliers and to make use of all information available at that epoch.

In particular, the MAD-based filter is obtained by applying the Hampel identifier [4],[13], which replaces the outlier-sensitive classical statistical indexes (mean and standard deviation), with the outlier-resistant median and median absolute deviation from the median, respectively.

As documented in [14], the median x^C of a generic data sequence is obtained by first rank-ordering it from smallest to largest, i.e.:

$$x_{(1)} \le x_{(2)} \le \ldots \le x_{(N-1)} \le x_{(N)} \qquad (1)$$

and then taking x^C as either the middle value (if N is odd) or the average of the middle two values (if N is even). The MAD scale estimate is then defined as:

$$S = 1.4826 \cdot median\left\{\left|x_k - x^C\right|\right\}, \qquad (2)$$

where the factor 1.4826 in Equation (2) is chosen so that the expected value of S is equal to the standard deviation σ for normally distributed data.

A rejection threshold t (with t as an integer positive value) is then introduced and if

$$\left|x_k - x^C\right| > t \cdot S \qquad (3)$$

x_k is declared an outlier and it is removed from the dataset.

Figure 2 shows an example of the general behaviour of both a classical 3σ dynamic filter and a MAD-based filter with a rejection threshold t =3 (hereafter named 3S MAD-based filter) for a small real dataset containing a great outlier.

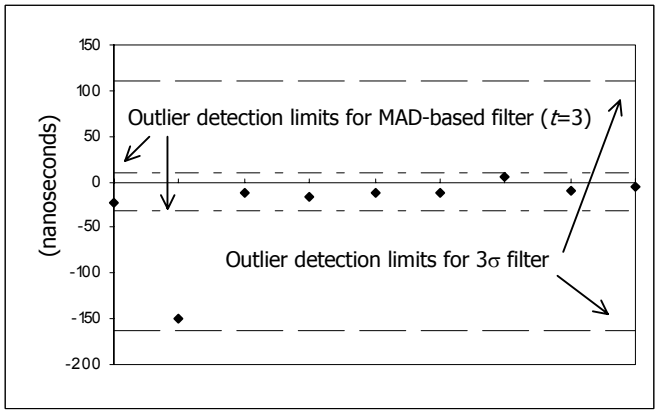

Figure 2: Behaviour of different filtering on a small real dataset containing a great outlier ($\cong 4\sigma$).

As it comes out observing the example reported in Figure 2, in general the 3S MAD-based filter seems to be a better choice than the classical 3σ filter, concerning the detection and removal of outliers especially when the parameters are estimated from a small data set (as in the case of epoch measurements), as also documented in literature [18],[14]. On the other hand, it is worth to notice that, for large datasets, the 3σ dynamic filter and the 3S MAD-based filter seem to provide the same performance, as confirmed by the values in Table 1, concerning the estimates of the mean and the standard deviation values.

Data set length	*Filter*	*Estimated*	
		Mean (ns)	*Std. Dev. (ns)*
89 samples	3σ	5.6	3.4
	3S MAD	5.6	3.4
9 samples	3σ	-25.9	47.1
	3S MAD	-10.4	7.9

Table 1: Effect of 3σ and 3S MAD filters on both a small dataset (epoch measurements of the example reported in Figure 2) and a large dataset (GPS daily measurements at IEN for MJD 52988).

Then, after the epoch-based filtering procedure, the average of all validated values is computed and only one datum per each epoch results. With the aim of removing any residuals anomalies caused mainly by the receiver along with its external reference (the UTC(k) time scale in case of metrological laboratories), a further 3σ filtering procedure is

then applied on the 24 hours interval of the considered day. As mentioned above, since the receiver could collect up to 90 measures on each day, both the MAD-based and the 3σ filter are comparable in term of outlier detection performance. The latter was selected for software implementation purposes.

Finally, the linear regression of all the mean-epoch values is computed for each 24 hours interval centred at 00h UTC of the considered day. This smoothing procedure has the capability to filter out the short-term instabilities noticed on the measures. Only one datum per day is then produced by the algorithm as the estimate of the mean offset between the local reference UTC(IEN) and either GPS time or other remote UTC(k) laboratories.

The estimated UTC(IEN) versus GPS time offset provided by the described algorithm is plotted in Figure 3 for the 2 months period from MJD 52640 (January 1st, 2003) to MJD 52698 (February 28th, 2003). As showed in the plot, the results coming from the processing algorithm are very close to those coming from the BIPM Circular T data, having residuals with 2.2 ns rms.

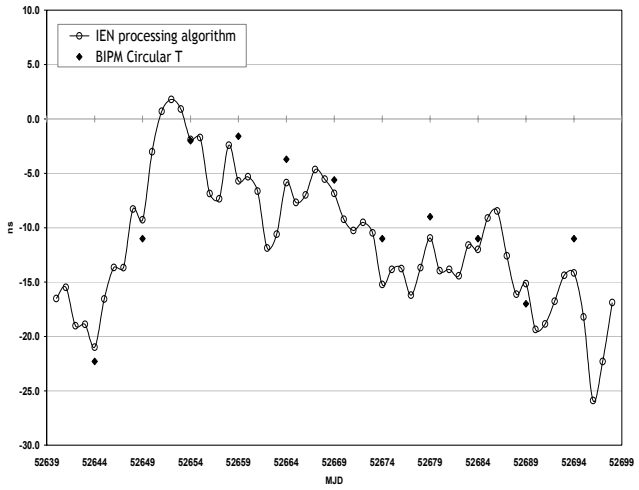

Figure 3: Behaviour of UTC(IEN) versus GPS time as estimated by the processing algorithm on the 3SN receiver data (January 2003 – February 2003). The same quantity as estimated by the BIPM Circular T data (5 days spaced) are also reported.

In case of time scale comparison with remote UTC(k) laboratories, the processing algorithm is quite different , even if it is based on three-stages too. In particular, the 3*S* MAD-based epoch filtering is now applied on the set of raw differences between the measurements of satellites in strict common view by the two laboratories.

As a consequence, the differences between raw measurements lead to remove all the "common" source of uncertainties. Besides, the further filtering on each epoch allows coping with anomalous asymmetrical common views between the two laboratories.

3 Receivers noise characterization

With the aim to characterize the noise and the stability of the IEN GPS receivers, the measurements provided by the two timing and the two geodetic GPS receivers have been processed using the MAD-based filter algorithm described in the previous section.

For a 3 months period from MJD 52988 (December 15th, 2003) to MJD 53079 (March 15th, 2004), the offset between UTC(IEN) and GPS time has been estimated from the data of each receiver. In particular, for the 3SN and the TTS timing receivers, weekly CGGTTS-formatted data files [2] have been considered. On the other hand, for the geodetic receivers ASH and JAV, the daily RINEX files [8] (containing phase and pseudorange dual-frequency measurements with 30 seconds sampling rate) have first been converted in 5-days CGGTTS-formatted files using specific software [6], as required in BIPM TAI P3 activities.

Figure 4 shows the time series of the offset UTC(IEN) versus GPS time, as one datum per day at the 0h UTC standard epoch.

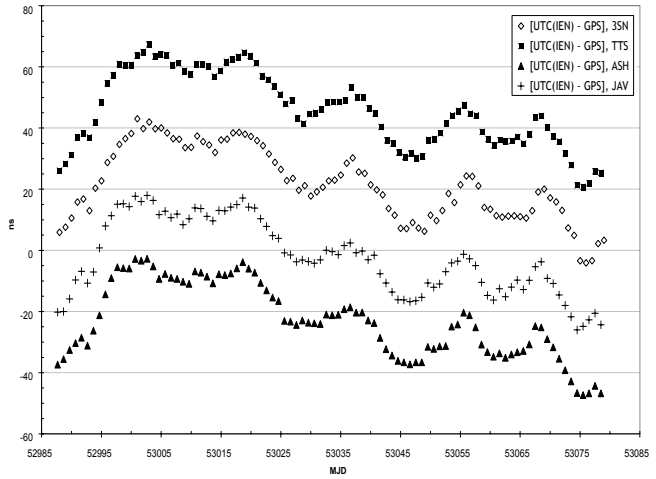

Figure 4: Behaviour of UTC(IEN) versus GPS time as estimated by different receivers (December 2003 – March 2004). A 20 ns offset has been added to JAV for purpose of plotting.

Since the JAV receiver was referenced by the free-running H-maser #1 operated by IEN (in the following HM1), the [HM1–GPS] offset resulting from the algorithm has been post-processed using the daily [UTC(IEN)–HM1] internal measurements, in order to remove the HM1 contribution. A costant bias equal to 140627 ns is also removed.

Apart from not compensated calibration biases (discussed later), the time series coming from different receivers seem to be very similar and consistent with the BIPM Circular T data. This is also confirmed by the day-by-day residuals reported in Figure 5, where some pairs of receivers have been taken into account.

Please note that such residuals have been estimated by a strict common view approach, instead of compare the daily values,

achieving a small improvement in term of data spreading. In this case, as mentioned in section 2, the processing algorithm jointly treats the two receivers and only the differences between the measurements of the same satellite at the same epoch are computed.

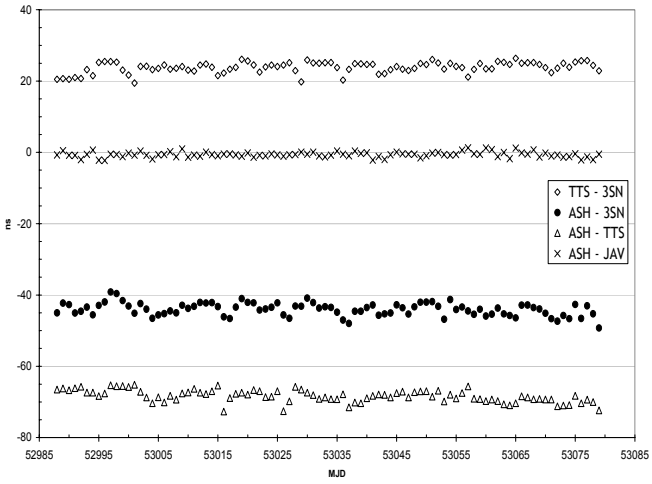

Figure 5: Time residuals between pairs of GPS receivers (December 2003 - March 2004)

Due to the UTC(IEN) "common clock" configuration of the receivers (native for 3SN, TTS and ASH, but also applicable for JAV after removing the HM1 contribution), the resulting residuals are intended to be the differential delay of pair of receivers. Table 2 reports the statistical indexes of such residuals, where the mean values are not significant in performance evaluation since there are calibration biases to be compensated. The corresponding frequency stabilities, in term of Allan deviations, are also given in Figure 6.

Receivers	*Mean (ns)*	*σ (ns)*
TTS - 3SN	23.8	1.6
ASH - 3SN	-44.0	1.8
ASH - TTS	-68.3	1.7
ASH - JAV	-0.6	0.8

Table 2: Statistical indexes for the time residuals between pairs of GPS receivers (depicted in Figure 5).

It is worth to notice that the results in Table 2 concern a pair of receivers, since the residuals can be computed only comparing the measurements provided by two receivers. If the receivers could be assumed identical and independent, the noise figure of each receiver could be estimated to be a factor $\sqrt{2}$ lower.

Looking at the plots in Figure 6, the Allan deviations show a behaviour close to a noise with a τ^{-1} slope: as expected, the residuals are only affected by the typical additive thermal noise of electronic devices (the receiver), since both the reference time scale and the GPS contributions have been removed by the processing procedure. Actually, an additional investigation using the modified Allan deviation detects both white phase (WP) and flicker phase (FP) noise components at all the averaging times, with different level, but only for the residuals involving timing receivers.

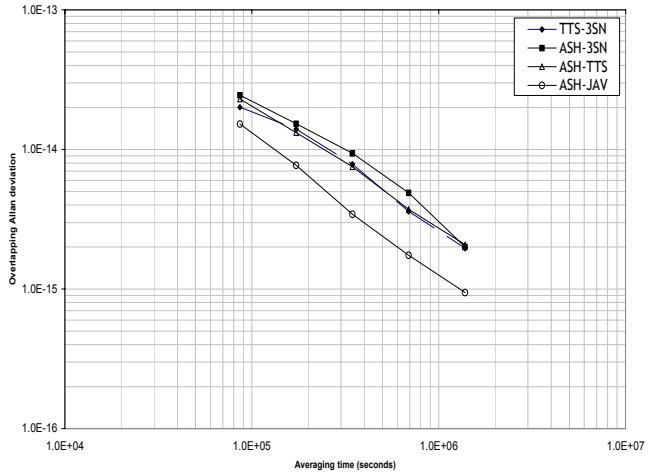

Figure 6: Allan deviation of the time residuals between pairs of GPS receivers (depicted in Figure 5).

In the last row of Table 2, the statistical indexes concerning the residuals for the two geodetic GPS receivers are also indicated, after removing the HM1 contribution. As well showed in Figure 5, both the classical variance and the Allan deviation in Figure 6 are a factor close to 2 lower than for either timing/timing (TTS-3SN) or timing/geodetic (ASH-TTS) pair of receivers. For instance, over 1 day, the Allan deviation decreases from $(2.3 \cdot 10^{-14} \cdot \tau^{-1})$ for ASH-TTS pair to $(1.5 \cdot 10^{-14} \cdot \tau^{-1})$ for ASH-JAV.

Furthermore, in case of geodetic/geodetic pair, the Allan deviation shows a pure WP noise for all the averaging times considered (up to 2 weeks) and no FP component is noticed. Then, it is possible to infer that using the P3 iono-free combination of the dual frequency P-code measurements provided by geodetic GPS receivers, the receiver noise could be estimated with higher accuracy, filtering out any other source of noise (such as, the measurement method itself).

4 A "geodetic-based" approach

The precise point positioning (PPP) is a post-processing approach using un-differenced dual frequency pseudorange and carrier phase observations coming from a single geodetic GPS receiver, together with the high-quality GPS products such as those provided by the International GPS Service (IGS) [9].

Taking advantage of the precise satellite clock estimates as well as the precise satellite coordinates in the IGS products, the PPP allows stand-alone point positioning (kinematic and static) with centimetre precision in term of station coordinates and receiver clock offset estimates with sub-ns precision.

It means that the PPP eliminates the need to acquire simultaneous observations from a reference station or a

network of tracking stations. As a consequence, the stand-alone position of a single geodetic GPS receiver can be autonomously estimated with cm precision, even if the receiver is not part of a network of stations (such as, the world wide distributed IGS network).

For a number of years, PPP algorithms have been available in the GIPSY [12] GPS analysis software and, more recently, in the BERNESE software [17].

In particular, since the mid-90's the PPP approach has been developed by the Geodetic Survey Division (GSD) of Natural Resources Canada (NRCan), which is one of the IGS Analysis Centers contributing daily predicted, rapid and final GPS orbits and clocks to the IGS for combination. The current NRCan PPP implementation [10] is available as an on-line application [3] and only requires the submission of a valid observation RINEX file to obtain a stand-alone position estimate, as well as station clock estimates and tropospheric zenith path delays.

4.1 PPP clock offset estimates evaluation

With the aim to validate the timing-oriented performance of the NRCan PPP software, an experimental activity is carried out at IEN since few months using the on-line service kindly provided by GSD NRCan.

Preliminary results are reported and discussed in the following, using a 9 days period from MJD 53026 (January 22nd, 2004) to MJD 53034 (January 30th, 2004). Since this time window is fully included in the 3 months period considered in the receivers noise analysis reported in Section 3, a direct comparison of classical GPS common view (based on 3SN and TTS timing receivers), iono-free P3 (using ASH and JAV geodetic receiver data, as converted in CGGTTS format) and geodetic-based (PPP) approaches is then available.

In our analysis, phase and pseudorange dual-frequency measurements have been collected from both geodetic receivers and formatted in daily RINEX files. These RINEX files have been then processed with the PPP software using IGS final products (available with two weeks latency), providing receiver clock offset estimates every 30 seconds. It is worth to mention that the precise satellite orbits and clocks estimates in the IGS final products are given with 15 minutes and 5 minutes interval, respectively, with an accuracy less than 5 cm/0.1 ns.

Let ASH_{PPP} and JAV_{PPP} these estimates for Ashtech and for Javad, respectively:

$$ASH_{PPP} = \{GPS - [UTC(IEN) + k_{ASH}]\} \quad (1)$$

$$JAV_{PPP} = \{GPS - [HM1 + k_{JAV}]\}, \quad (2)$$

where k_{ASH} and k_{JAV} are the delays of the receiver internal references versus UTC(IEN) and HM1 external reference signals, respectively.

Subtracting the two estimates (1) and (2), at the same epochs, results in the offset of UTC(IEN) versus the free-running HM1, except for the differential delay (k_{ASH} - k_{JAV}) of the two receivers:

$$JAV_{PPP} - ASH_{PPP} = [UTC(IEN) - HM1] + (k_{ASH} - k_{JAV}). \quad (3)$$

The time series of the offset (3) is reported in Figure 7, after removing a quadratic trend (a = 0.3 ns/day^2; b = 51.2 ns/day; c = 143 609 ns). As showed by the Allan deviation in Figure 8, the residuals are very similar to a typical behaviour of a commercial Cs standard, which UTC(IEN) is based on.

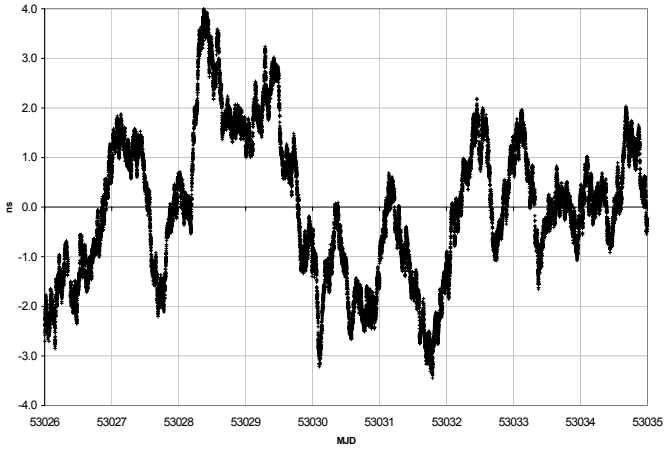

Figure 7: Time residuals between the Ashtech and the Javad receivers (January 22nd to January 30th, 2004), representing UTC(IEN)–HM1. Quadratic fit removed: a=0.3 ns/day^2; b=51.2 ns/day; c=143 609 ns.

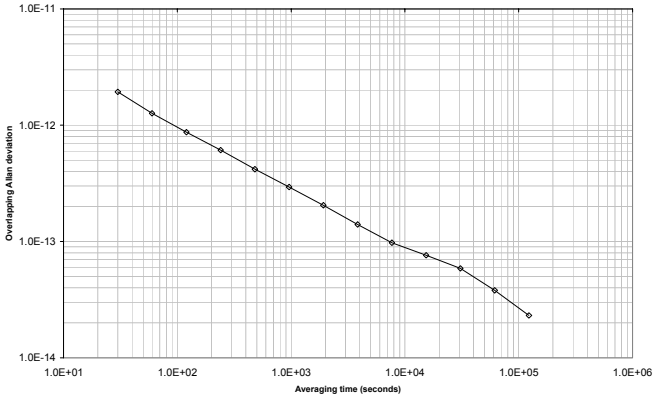

Figure 8: Allan deviation of the time residuals in Figure 7 between the PPP solutions for the Ashtech and the Javad receivers (January 22nd to January 30th, 2004), representing UTC(IEN)–HM1.

Moreover, in order to extract from Equation (3) the differential delay of the two receivers, the hourly [UTC(IEN)–HM1] values provided by the measurement system of IEN Time and Frequency Laboratory and the (JAV_{PPP} – ASH_{PPP}) estimates at each hour have been subtracted at the same epochs. A constant bias equal to 140603.3 ns is further removed, assuming it as the mean differential delay of the two receivers.

As plotted in Figure 9, the resulting hourly residuals are all in the range of –1.0 ns and 1.5 ns with a zero mean value (being removed the constant bias) and a 0.35 ns standard deviation.

Looking at the results in Table 3, the PPP geodetic approach seems to provide a stability performance better than that provided by both a classical common view approach on timing GPS receivers and a P3-based common view approach using the same geodetic GPS receivers.

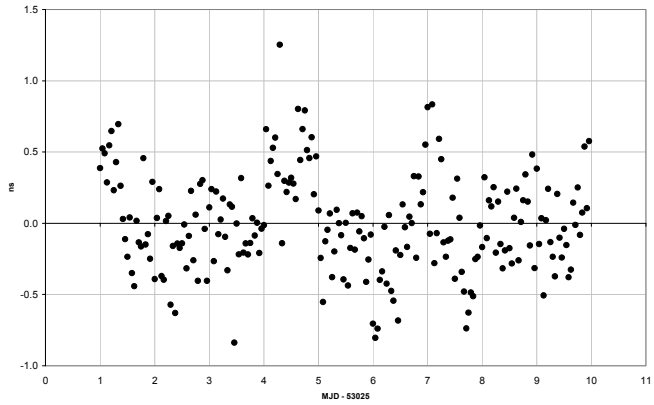

Figure 9: Time residuals of the differential delay between Ashtech and Javad receivers as estimated by PPP (January 22nd to January 30th, 2004). Constant bias removed: 140603.3 ns (mean differential delay).

Receivers	σ *(ns)*	$\sigma_y(\tau)$ @ τ = *1 day*
3SN – TTS via GPS CV	1.6	$2.0 \cdot 10^{-14}$
ASH - JAV via P3 (CGGTTS)	0.8	$1.5 \cdot 10^{-14}$
ASH - JAV via PPP	0.3	$0.8 \cdot 10^{-14}$

Table 3: Statistical index (classical standard deviation) and Allan deviation over 1 day for the time residuals of the differential delay between Ashtech and Javad receivers (depicted in Figure 9), compared with similar index previously reported in Table 2.

Moreover, the following Figure 10 reports the Allan deviation of the residuals of the two geodetic receivers as computed both via P3 (τ_0 = 1 day) and via PPP (τ_0 = 1 hour), where the stability performance improvement is well depicted.

Such result is mainly due to the use of dual frequency carrier phase measurements in the PPP algorithm, as well as the availability of high-quality GPS products (precise satellite clocks and orbit information) as provided in near real time by IGS.

However, it is worth to notice that the noise affecting PPP residuals has not the expected τ^{-1} slope (WP/FP) for all the averaging times. In effect, looking at the bottom line in Figure 10, a significant change in slope is observed for averaging times close to half a day. This issue has been already noticed in [11] and it is currently under inspection with the helpful support of the Canadian GSD.

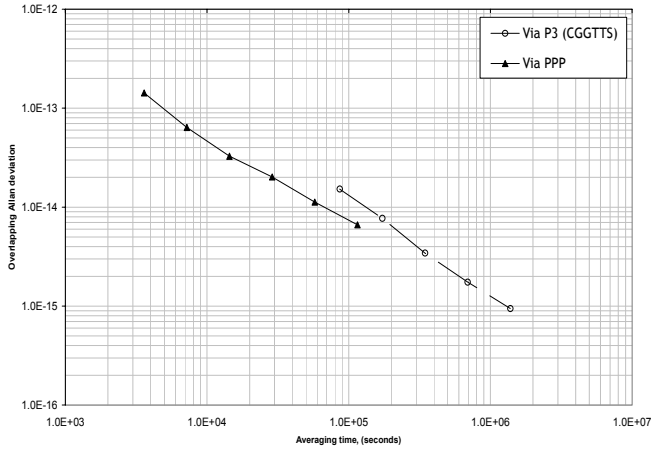

Figure 10: Allan deviation of the time residuals of the differential delay between Ashtech and Javad receivers as estimated by both PPP and P3 (January 22nd to January 30th, 2004).

4 Time transfer link between IEN and PTB using PPP

Relying on the promising results, the PPP method has then been used in the frame of a European link between the two metrological institutes, IEN and the Physikalisch-Technische Bundesanstalt (PTB), Braunschweig, Germany, in order to test its time transfer capability.

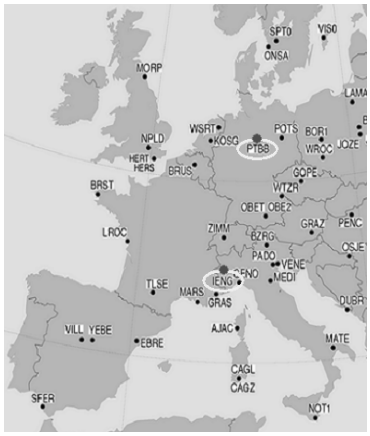

Figure 11: The European link between IEN and PTB metrological institutes.

Over such a link, two other time transfer methods (namely the TWSTFT and the GPS Common View) are regularly operated and a direct comparison of different synchronisation systems can then be achieved. In addition, the Ashtech Z12-T receivers of both laboratories are part of the IGS network (named IENG and PTBB, respectively).

For a 2 months period from MJD 53005 (January 1st, 2004) to MJD 53064 (February 29th, 2004), the daily RINEX files of

the receivers of the two laboratories have been reduced with the PPP software using IGS final products of precise satellite clocks and orbits. The resulting 30 seconds estimates have been compared, at the same epoch, and the differences have been then linear fitted (over 1 day) to have the best daily estimates at 0h UTC standard epoch.

It is worth to notice that the data coming from the above processing represent [UTC(IEN) – UTC(PTB)] except for the differential delay of the configuration of the two receivers hosted by IEN and PTB. Such a bias has been estimated with respect to the recent calibrated TWSTFT link between the two laboratories and a calibration value of –514.4 ns (σ = 1.1 ns) has then to be considered in the PPP link between IEN and PTB.

The time series of the calibrated PPP estimates is shown in Figure 12, together with the daily [UTC(IEN) – UTC(PTB)] offset as provided by the TWSTFT and the GPS CV. In addition, the same offset as computed using the BIPM Circular T data are also reported.

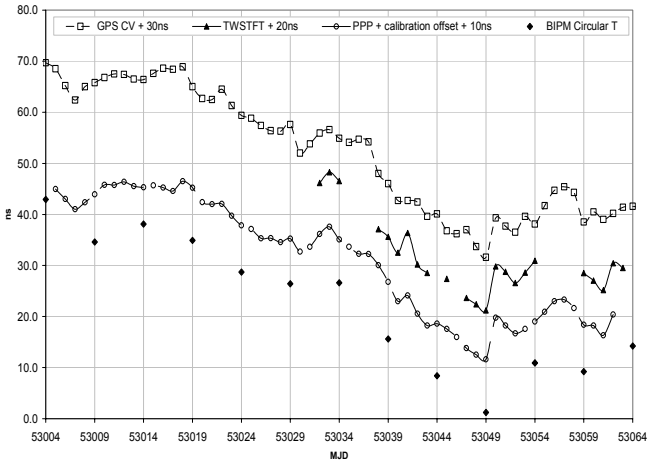

Figure 12: Behaviour of UTC(IEN) versus UTC(PTB) (January 2004 – February 2004) as provided by TWSTFT, GPS CV and PPP. The BIPM Circular T data (5 days spaced) are also depicted. An arbitrary offset is added to each series for purpose of plotting.

The residuals of the PPP estimates with respect to both TWSTFT and GPS CV are plotted in the following Figure 13.

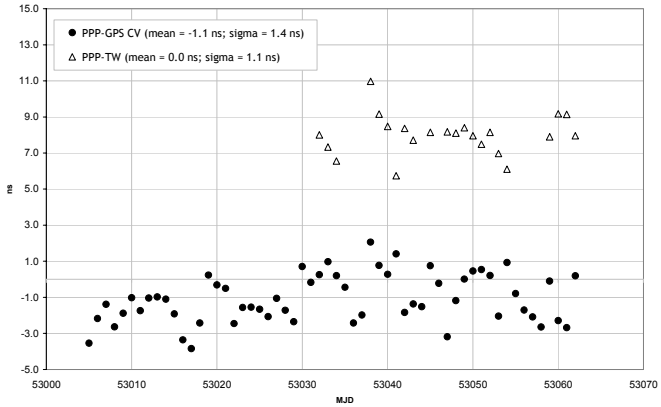

Figure 13: Time residuals of the PPP estimates (as corrected for the calibration bias computed using TWSTFT) with respect to both TWSTFT and GPS CV. An offset of +8 ns is added to the PPP-TW series for purpose of plotting.

As mentioned before, since January 2004 the ASH receiver is qualified as a permanent station of both EPN (EUREF Permanent Network) and IGS networks. The RINEX data from the receiver are regularly processed by some of the IGS Analysis Centers and they are also contributing to the IGS time scale [16].

In this frame, the clock products are daily available reporting the estimated behaviour of the clock driving the receiver (that is, UTC(k) in our case). Figure 14 shows a first comparison between IEN and PTB time scales (over a 5 days period), as estimated using the PPP approach and the IGS clock products (realigned to both rapid and final IGS time scale). Please note that, for purpose of plotting, an offset is added to each series.

Looking at the actual differences of the three time series, in term of accuracy, the PPP processing results are consistent at sub-ns level with the estimates from IGS which are based on a "network solution". In detail, the residuals show σ = 0.2 ns for PPP versus rapid IGS time scale, IGRT, and σ = 0.1 ns versus the final IGST, over a 5 days period.

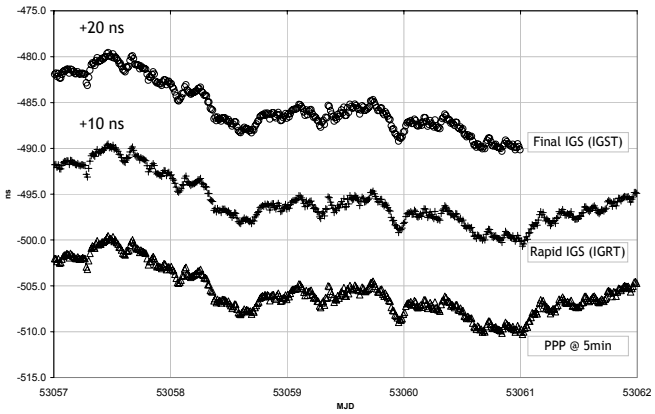

Figure 14: Behaviour of UTC(IEN) versus UTC(PTB) (22nd to 27th February, 2004) as estimated using PPP, Rapid IGS (IGRT) and Final IGS (IGST). The offsets shown in the graph are added to the series for purpose of plotting.

6 Conclusions

The operation and the noise characterization of the IEN GPS receivers (both timing and geodetic) have been addressed in this paper. The GPS measures are firstly treated by a IEN processing algorithm aiming to detect the outliers and to provide a robust, smoothed, daily estimates. From the analysis of the experimental results, it appears that the noise affecting GPS measures is close to $\sigma_y(1\ \text{day}) \cong 2 \cdot 10^{-14}$ when using timing receivers but it can be halved when using geodetic receivers with a TAI P3 like approach.

In addition, preliminary timing performance of the NRCan PPP geodetic approach have been presented, mainly focused on the estimation of the differential delay of two co-located geodetic GPS receivers (an Ashtech Z-12T and a Javad Legacy). Looking at the results, the PPP seems to provide a good stability performance over short/medium term, even better than that provided by both a classical common view approach on timing GPS receivers and a P3-based common view approach using the same geodetic GPS receivers.

The PPP has been also tested on the European link between IEN and PTB, where other time transfer methods (such as the TWSTFT and the GPS CV) are operated. After performing a calibration with respect to the recent calibrated TWSTFT link, the estimates provided by PPP are consistent with both the BIPM Circular T and the other time transfer methods with accuracy better than 2 nanoseconds.

Finally, concerning the same time transfer link between IEN and PTB, the PPP results are consistent (at sub-ns level) with the estimates carried out using the IGS clock products, which are available since the two metrological institutes are part of the IGS world wide network.

Acknowledgements

On behalf of the Istituto Elettrotecnico Nazionale "Galileo Ferraris", the authors wish to thank the Geodetic Survey Division, Natural Resources Canada (NRCan) for providing the GPS Precise Point Positioning (PPP) software. Special thanks to François Lahaye (NRCan) for kind support and helpful advices provided on the usage of PPP software.

The authors are also grateful to Andreas Bauch (PTB, Germany) and his staff for making available GPS CV data as well as RINEX data for PTBB IGS station. Special thanks to our colleague L. Lorini for providing TWSTFT data as well as to the students with the Time and Frequency Laboratory for the helpful support in data retrieving and processing.

References

[1] D.W. Allan, C. Thomas, "Technical Directives for Standardization of GPS Time Receiver Software", *Metrologia*, **31**, pp. 69-79, (1994).

[2] J. Azoubib, W. Lewandowski, "CGGTTS GPS/GLONASS Data Format Version 01", *VII CGGTTS Meeting*, (1998).

[3] Canadian Space Reference System (CSRS) – Precise Point Positioning (PPP) on-line service, *Geodetic Survey Division (GSD) of Natural Resources Canada (NRCan)*, http://www.geod.nrcan.gc.ca/index_e/products_e/services_e/ppp_e.html.

[4] L. Davies, U. Gather, "The identification of multiple outliers", *J. Amer. Statist. Assoc.*, pp. 782-801, **vol. 88**, (1993)

[5] P. Defraigne, G. Petit, C. Bruyninx, "Use of Geodetic Receivers for TAI", *Proceedings of the 33rd Annual Precise Time and Time Interval (PTTI) Meeting*, Long Beach, California, pp. 341-348, (2001).

[6] P. Defraigne, C. Bruyninx, "Time Transfer for TAI Using a Geodetic Receiver; An Example with the Ashtech ZXII-T", *GPS Solutions*, pp. 43-50, **vol. 5 n. 2**, (2001).

[7] G. Graglia, E. Detoma, F. Cordara, R. Costa, L. Lorini, D. Orgiazzi, V. Pettiti, P. Tavella, J. Hahn, "The Experimental Precise Timing Station and the Galileo System Time generation in the Galileo System Test Bed Phase V1", *Proceedings of GNSS 2003 – The European Navigation Conference*, Graz, Austria, (2003).

[8] W. Gurtner, "RINEX: The Receiver Independent Exchange Format Version 2.10", (2002).

[9] J. Kouba, "A Guide to Using International GPS Service (IGS) Products", *IGS Central Bureau*, ftp://igscb.jpl.nasa.gov/igscb/resource/pubs/GuidetoUsingIGSProducts.pdf, (2003).

[10] J. Kouba, P. Héroux. "Precise Point Positioning Using IGS Orbits and Clock Products", *GPS Solutions*, **vol. 5 n. 2**, (2001).

[11] F. Lahaye, P. Collins, J. Popelar, "The Virtual Reference Clock (VRC) Time Scale of the NRCan Real Time Wide Area GPS Correction Service (GPS·C)", *IV International Time Scales Algorithm Symposium*, Sèvres, France, (2002).

[12] S. M. Lichten, Y. E. Bar-Sever, E. I. Bertiger, M. Heflin, K. Hurst, R. J. Muellerschoen, S. C. Wu, T. P. Yunck, J. F. Zumberge, "GIPSY-OASIS II: A High precision GPS Data processing System and general orbit analysis tool", *Technology 2006, NASA Technology Transfer Conference*, Chicago, Il., (1995).

[13] R.K. Pearson, "Exploring process data", *J. Process Contr.*, pp. 179-194, **vol.11**, (2001)

[14] R.K. Pearson, "Outliers in Process Modelling and Identification", *IEEE Transactions on Control Systems Technology*, **vol. 10**, pp. 55-63, (2002).

[15] J.R. Ray, "IGS/BIPM Time Transfer Project", *GPS Solutions*, pp. 37-40, **vol. 2 n. 3**, (1999).

[16] J. Ray, K. Senior, "IGS/BIPM pilot project: GPS carrier phase for time/frequency transfer and timescale formation", *Metrologia*, **40**, pp. S270-S288, (2003).

[17] M. Rothacher, L. Mervart, "The Bernese GPS Software Version 4.0", *Astronomical Institute, University of Berne*, Berne, Switzerland, (1996).

[18] D.F. Vecchia, J.D. Splett, "Outlier - Resistant Methods for Estimation and Model Fitting", *Proceedings of the Workshop Advanced Mathematical Tools in Metrology*, Torino, Italy, pp. 143-154, (1993).